IJIE

The International Journal of Integrated Engineering

Microstructural Analysis of Strain Rate Dependence for Commercial Dual Phase Steel DP590 Undergoing Finite Strain Deformation

M. F. Kamarulzaman[1], M. K. Mohd Nor[1,2*], M. S. A. Samad[1,2]

[1]Faculty of Mechanical and Manufacturing Engineering,
 Universiti Tun Hussein Onn Malaysia, Parit Raja, Batu Pahat, 86400 Johor, MALAYSIA

[2]Computer Aided Engineering, Vehicle Performance, Group Research and Development, PROTON Holdings Bhd,
 Shah Alam, MALAYSIA

Abstract: This paper analyses the correlation of strain rate dependency of the material with sheet metals manufactured orientation that would influenced the microstructural changes in terms of martensite-ferrite and voids characteristics. The investigation on the deformation behaviour of Advanced High Strength Steel (AHSS) DP 590 was conducted using a uniaxial tensile test along the two principal directions that is through longitudinal (0°) and transverse (90°) through the strain rates of $1x10^{-1}s^{-1}$ to $1x10^{-4}s^{-1}$. This allows for a strain rate dependency analysis conducted via stress-strain curve development. Scanning Electron Microscope (SEM) is used to examine the deformed microstructure for micro structural behaviour and for the void analysis on the number of voids and the average void sizes. Referring to the stress-strain curve, it is shown that the mechanical properties of the specimen behaved differently at those preferred orientations and are sensitive to the changes in the loading conditions. This could be observed as the DP590 at 0^0 of rolling direction have higher stiffness value as compared to the 90° of transverse direction, the variant of the response of the material could be observed to be mildly anisotropically inclined instead of behaves as an isotropically behaved material. The response is also observable within the deformed microstructure. For instance, the higher strain rate indicates a higher number of voids, with a larger average void sizes, from this response it is observed the changes of the strain rate of the material would affect the material behaviour. As for the ferrite-martensite analysis, it could be observed in both different material orientations that as the lower strain rate was applied to the specimen, the strength of the material tends to become weaker since the martensite island becomes smaller at smaller strain rate levels.

Keywords: Dual-Phase Steel DP590; finite strain deformation; strain rate dependence; microstructural analysis; uniaxial tensile test

1. Introduction

Dual-Phase (DP) metal sheets in recent years are being used extensively throughout the automotive industries, which are formed into energy absorption materials that include multiple different sizes and shapes for their products. As a common practice within the industry to consider these materials as a totally isotropic material meanwhile it didn't represent the accurate representation of the material behaviour at all. DP metal sheets are one of the materials that in recent years have been identified as behaving anisotropically as to the normal standard assumption. It is a fundamental definition to be concluded as the materials in question would affect the simulation outcome for the said material within a controlled environment since it needed to be treated as an orthotropic material. This had been observed within other materials as example the fibre-reinforced elastomers or glassy polymers. While under large elastoplastic deformation,

the material exhibits orthotropic behaviour while undergoing large elastoplastic deformation [1]. This is due to the preferential orientation of the material itself after undergoing multiple different manufacturing processes [2]. While the material in a quasi-static rates of strain which had been recorded before [3],[4],[5],[6],[7] the behaviour of metals that impacted with dynamic shock loading can be found in Smallman [8], Gray et al. [9], Mohd Nor et al. [10], Mohd Nor et al. [11] and Mohd Nor et al. [12],[1]. Advanced High Strength Steel (AHSS) had been a common use within the industry as a DP steel sheet metal consists of a ferrite and martensite multi-phase microstructure and martensite embedded within it would have it behaving orthotopically. This is mainly due to the fact that the material had undergone multiple different treatments prior to it being formed, also simulated with the behaviour as being under plastic deformation [21]. Meanwhile, their high ductility and strength also contributes as a factor as to why DP steels are being commonly accepted as compared to other conventional steel grades. The flexibility of the material's volumetric fractions and the strength of martensite also contribute a good combination of strength and formability since it increases with strength proportional to the materials' martensite fraction while increased in ductility and ductility strain hardening when ferrite fraction are increased. The crucial observation also has been made towards DP steel behaviour as it would depend on strain rates, temperatures, and material rolling orientations [13],[14]. This would indicate that the material would not behave consistently throughout, after being treated with multiple different parameters as mentioned thus are being discussed within this study as DP steel would deform through dislocation from gliding what happens within the soft ferrite matrix. When a high strain-hardening rate of DP steels happens, the strain is concentrated in the ferrite matrix, which is a crucial indicator for both the volume martensite-ferrite phase of the material [15]. By approaching the tension experiments, we could observe the response related to the microstructure evolution of the DP steels as these materials are being formed into different shapes for the automotive parts within the production line. This same approach is adopted later within this study. It is noted that the fatigue strength of the steel's tensile strength are dependent on the material's orientations and strain rate that would, in turn influence the microstructural response of the DP steel. This response will be captured by using the SEM (scanning electron microscope) analysis from the microstructural changes and microstructural defects through microstructural void analysis. This study uses a typical DP steel that is DP590 with its typical mechanical properties being present within Table 1 as a reference. Even though the extensive study had been previously conducted, there are still a complete gap in mechanical behaviour characterisation that represents the following parameters in table 1 even though being widely accepted. Regardless, it had only provided with only a few characteristics without the damage characteristics of the materials at different strain rates.

Table 1 - Properties of DP590 (Junehyung Kim et al. 2009) [20]

Yield strength (MPa)	Ultimate Tensile strength (MPa)	Young's modulus (GPa)	Poisson's ratio (v)
409.3 - 420	568.4 - 591.5	210	0.3

2. Methodology

The experimental testing that was conducted following ASTM E8 is discussed in this section. A rolled plate of DP590 was supplied by the national automotive manufacturer PROTON Bhd. The specimen was formed from the two different sheets that are the longitudinal (rolling direction, 0°) and transverse (90°) directions. In order to observe the behaviour of the specimen that undergoes a finite strain deformation is by conducting uniaxial tensile testing as it provides sufficient data for material characterisation [6]. The specimens are formed into 12 different specimens for each sheet metal that was provided according to their material orientations with different strain rates as explained in table 3 provided for the experimental design. The materials are prepared according to the geometry from the ASTM E8 shown in Table 2 and Figure 2. Figure 1 and Table 3 show the example of tensile specimen ASTM E8 and the specimen matrix in this study, respectively. With this, the plastic properties of DP590 was obtained.

3. Result and Discussion

The response of DP590 subjected to various strain rates is discussed in this section in terms of stress-strain curves and microstructural analyses. The microstructural analysis is conducted to review martensite-ferrite response, including voids characterisation towards strain rate changes. These analyses are important specifically for the ductile and unique microstructure of DP steels since the stress-strain curves represent the graphical measure of material's mechanical properties that is strongly influenced by the microstructural changes in the materials. Tensile and SEM machines used in this work are shown in Figures 3 and 4, respectively.
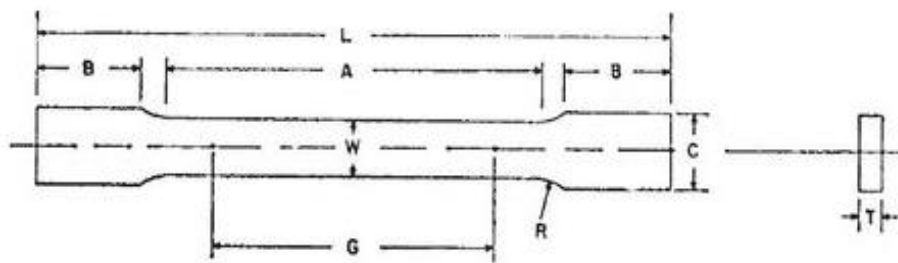
Fig. - 1 Example of tensile specimens

Fig. 2 Specimen's dimension

Table 2 - Specimen's measurements

Parameter	Size (mm)
Gage Length, G	25.0
Width, W	6.0
Thickness, τ	1.0
Radius of fillet, R	6.0
Overall length, L	100.0
Length of reduced section, A	32.0
Length of grip section, B	30.0
Width of grip section, C	10.0

Table 3 - Specimen matrix

Cross Head Speed (mm/min)	Strain Rate (s^{-1})	Rolling Direction $(^0)$
0.15	1×10^{-4}	0
		90
1.5	1×10^{-3}	0
		90
15	1×10^{-2}	0
		90
150	1×10^{-1}	0
		90

3.1 Stress-Strain Curves

The stress-strain curves in the longitudinal and transverse directions are shown in Figures 5. Generally, the material is sensitive to strain rate [20],[21]. It is observed that flow stress correlates with the strain rate. This behaviour can be clearly observed within the plastic region of the curves and look more obvious in the transverse direction. The flow stress is also higher in the longitudinal direction compared to the transverse direction, and consistent in all strain rates. From each of the graph presented in Figure 5, it is observed that the flow stress correlates with the strain rate. This behaviour can clearly be analysed that the higher the strain rate is, the higher the trend of the flow stress would be. If we compare the flow stress, Elasticity, E, Stiffness, σ, and the material's ultimate tensile strength (UTS), according to the principal rolling direction of the sheet metal, longitudinal (0°) direction tends to be higher compares to the transverse (90°) direction

[14]. As stated above, the stiffness of the material is observed behaving as the higher the strain rate would be, the higher the value of yield stress, σ which means that the stiffer the material would be. These are observed at strain rate 1×10^{-4} s^{-1}, 1×10^{-3} s^{-1}, 1×10^{-2} s^{-1}, and 1×10^{-1} s^{-1} with the value of 346 MPa, 355 MPa, 364 MPa, and 371 MPA respectively for longitudinal directions meanwhile, (1×10^{-4} s^{-1}) 344 MPa, (1×10^{-3} s^{-1}) 361 MPa, (1×10^{-2} s^{-1}) 363 MPa, and (1×10^{-1} s^{-1}) 370 MPa for transversal directions respective to the strain rate of the materials.

Fig. 3 - Tensile machine - ZWICK Roell Z0100

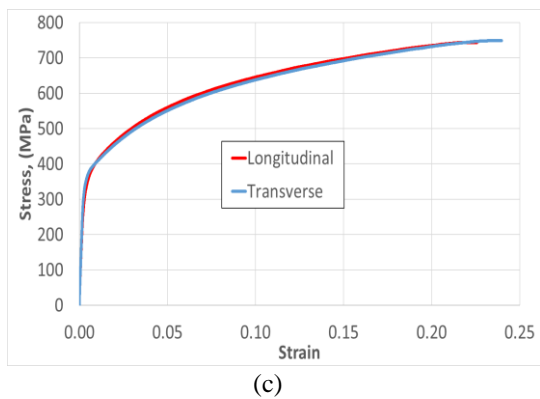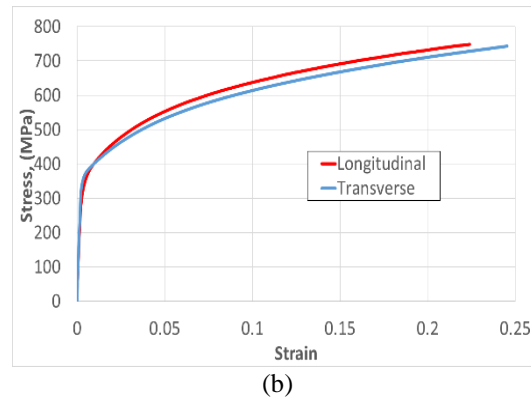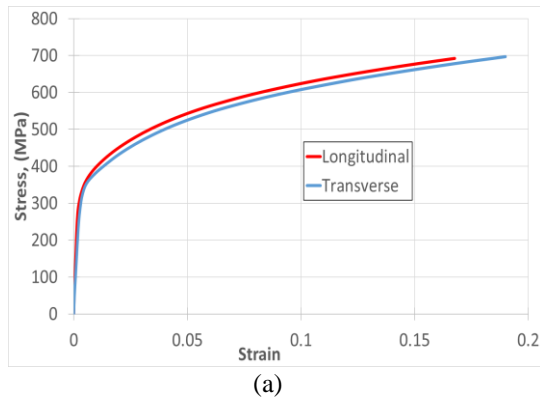**Fig. 4 - Scanning Electron Microscope (SEM) machine - JOEL JSM-630LV**

(a)

(b)

(c)

(d)
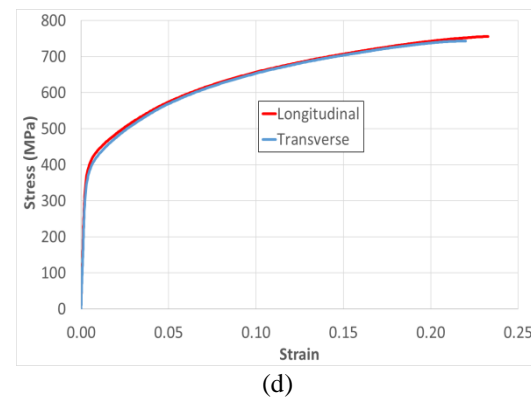
Fig. 5 - Stress-strain curve in different direction at various strain rate: (a) 1×10^{-4} s^{-1}; (b) 1×10^{-3} s^{-1}; (c) 1×10^{-2} s^{-1}; (d) 1×10^{-1} s^{-1}

The elasticity of the material were analysed through the value of Young's Modulus, E, as for longitudinal direction are (1×10^{-4} s^{-1}) 186.74 GPa, (1×10^{-3} s^{-1}) 189.27 GPa, (1×10^{-2} s^{-1}) 192.52 GPa, and (1×10^{-1} s^{-1}) 193.14 GPa respectively. These were compared to the transversal direction with the value of (1×10^{-4} s^{-1}) 185.39 GPa, (1×10^{-3} s^{-1}) 188.28 GPa, (1×10^{-2} s^{-1}) 191.10 GPa, and (1×10^{-1} s^{-1}) 192.69 GPa respectively. It is observed that the higher the strain rate, the higher the value of the Young's Modulus, and the longitudinal rolling direction generally has a higher elasticity as

compared to the transverse rolling direction. The material's ductility is also being analysed in the value of UTS as it was noted that ductility correlated to UTS of the material [22], for longitudinal direction are (1×10^{-4} s^{-1}) 744 MPa, (1×10^{-3} s^{-1}) 761 MPa, (1×10^{-2} s^{-1}) 744 MPa, and (1×10^{-1} s^{-1}) 751 MPa respective to the strain rate. While for transverse directions are (1×10^{-4} s^{-1}) 748 MPa, (1×10^{-3} s^{-1}) 754 MPa, (1×10^{-2} s^{-1}) 749 MPa, and (1×10^{-1} s^{-1}) 743 MPa respectively. It is observed that the value of the UTS would increase as the strain rate increases, and the longitudinal direction is observed to be inconclusive compared to the transverse directions. All recorded values and data obtained from the experiment is summarised in Table 4.

Table 4 - Tensile value at different strain rates and orientation

Material Direction	Strain Rate (s^{-1})	Young's Modulus (GPa)	Yield Stress/ Strength (MPa)	UTS (MPa)
0°	1×10^{-4}	186.74	346	744
	1×10^{-3}	189.27	355	761
	1×10^{-2}	192.52	364	744
	1×10^{-1}	193.14	371	751
90°	1×10^{-4}	185.39	344	748
	1×10^{-3}	188.28	361	754
	1×10^{-2}	191.10	363	749
	1×10^{-1}	192.69	370	743

3.2 Martensite-Ferrite Analysis

Within this section of the damage analysis, the damage mechanisms that are happening within the experiment boundaries are being observed as before and after the tensile test had been conducted. The following figures are observed microstructure for the AHSS DP590 at Longitudinal and transversal direction with different strain rates. The micrographs in Figures 6 to 10 capture large ferrite grains slip-bends, and it appears that smaller sizes tend to slip and cross over to the ferrite or martensite rich grains. These slip bends that are observed tend to develop localised deformation bends that it ran through within the microstructure despite it being barely noticeable between the different orientational directions. Even so, the transverse direction has a lower mechanical strength as compared to the longitudinal counterpart.
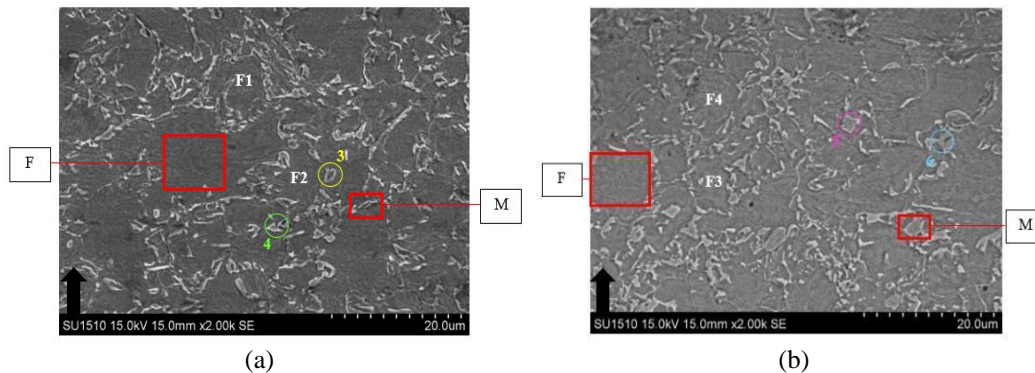

Fig. 6 - Undeformed AHSS DP590 Microstructure for (a) Longitudinal; (b) Transverse

Martensite islands can deform in either tensile, shear, or bending that depends on their loading direction, morphology, and deformation state of the surrounding ferrite grains according to Ghadbeigi et al. [16]. The deformation of the grain through bending and tensile as labelled in 3 are captured without any pronounced elongation towards the loading direction as indicated by the black arrow from the figures. As the strain rate of the material increases, the material's strength becomes increasingly pronounced as the martensite island's size increases and ferrite region slip bends decrease. The micrograph in Figure 11 shows that the failure mechanism of the martensite in the DP steel shows the extent of deformation in their phase boundaries. As indicated, there are not enough evidence of decohesion at the phase boundaries even as the martensite islands fracturing began to occur. The longitudinal diagram section of the figure (a), (b), (c), and (d), exhibits local necking (labelled 4) in the martensite island and the micro-cracks are initiated from both sides of the narrow central region DP590 has adjustable volumetric fractions and the strength of martensite thus exhibit combination of formability and strength [16].
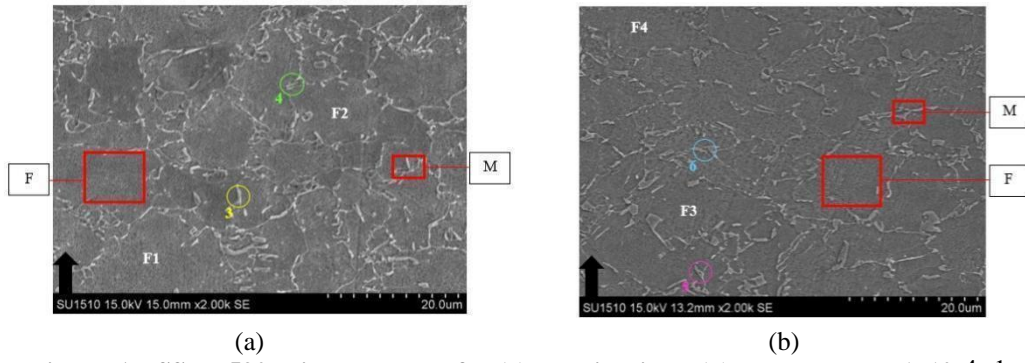
(a)   (b)

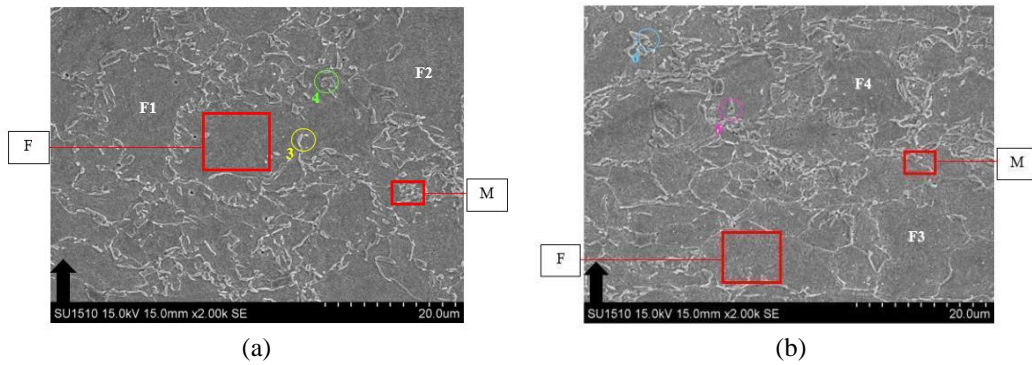**Fig. 7 - AHSS DP590 Microstructure for (a) Longitudinal; (b) Transverse at 1×10^{-4} s^{-1}**

(a)   (b)

Fig. 8 - AHSS DP590 Microstructure for (a) Longitudinal; (b) Transverse at 1×10^{-3} s^{-1}
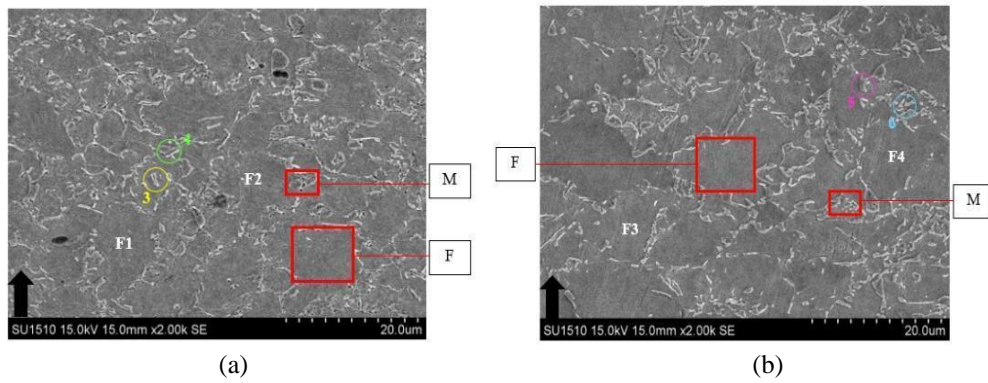

(a)   (b)

Fig. 9 - AHSS DP590 Microstructure for (a) Longitudinal; (b) Transverse at 1×10^{-2} s^{-1}
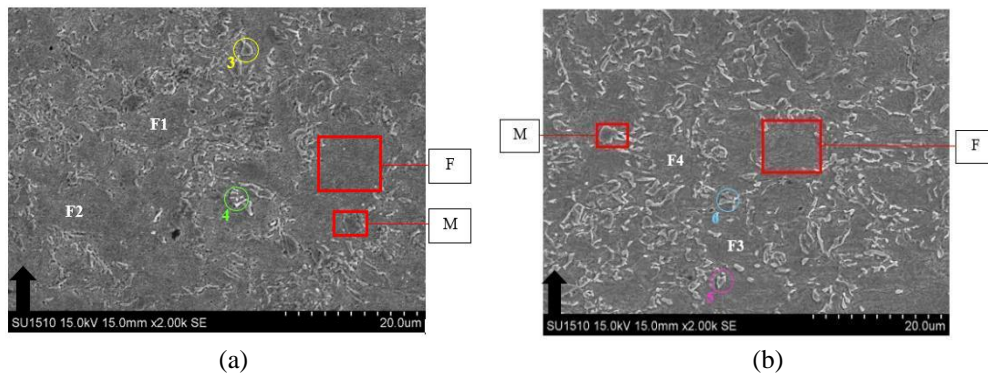

(a)   (b)

Fig. 10 - AHSS DP590 Microstructure for (a) Longitudinal; (b) Transverse 1×10^{-1} s^{-1}
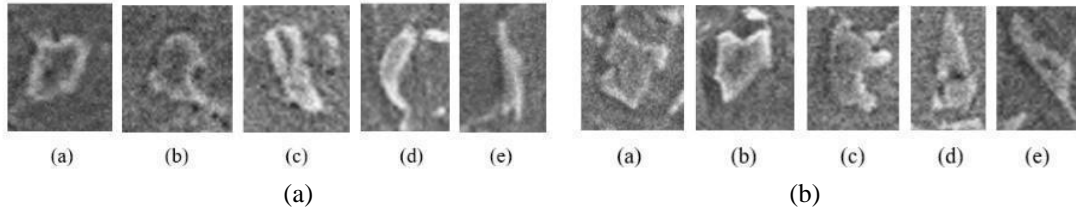
(a)   (b)

Fig. 11 - Deformation and crack initial in martensite islands (a) Longitudinal; (b) Transverse

Besides, the significant ductility and strain hardening also can be shown after yielding as the mobile dislocation density increases in a softer phase which is called ferrite. With closer inspection, the nodes that had been identified have no discernible decohesion at their phase boundaries. It is observed that ferrite rich regions tend to slip bands at lower strain levels which in turn have lower strength of material while martensite island's become smaller in size at lower strain levels. All of these behaviours are present within both of the rolling directions of the materials, longitudinal and transverse directions.

3.3 Voids Characterization

The quantitative analysis of the data are compiled within the number of voids and average size of voids as a function of different strain rates, as shown in Figure 12. The data is compared with the pre-deformation of the specimen at room temperature to obtain a better view of the correlating factors of the void density and size towards strain rate changes.

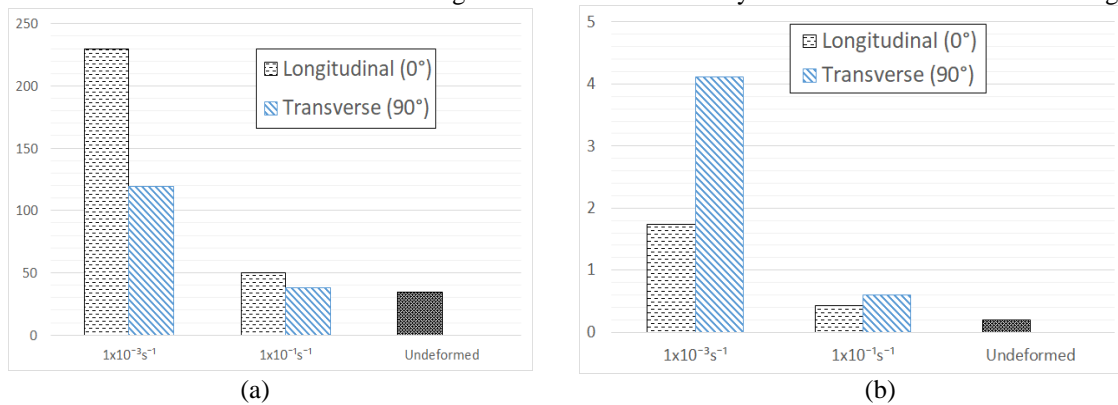(a)   (b)

Fig. 12 - Analysis summary from ImageJ for DP590: (a) Number of voids from different directions and strain rate; (b) Average void size from different directions and strain rate

The data acquired from the void size shows that the number of voids present at a lower strain rate 1×10^{-3} are much higher compared to higher strain rate 1×10^{-1}. Generally, there are 131,076 μm^2 difference along the longitudinal, and 351,256 μm^2 difference within the rolling directions. A similar pattern of void density is also shown between both strain rates of the specimen. 22,943 units of voids are obtained within the longitudinal direction at 1×10^{-3} strain rate, and 4,965 units of voids are observed at 1×10^{-1} strain rate. Further, along the transverse direction, 11,896 units are observed at 1×10^{-3} strain rate, and 3,820 units 1×10^{-1} strain rate. with a difference of 8,076 units of voids present.

3.4 Damage initiation and progression

The above Figures 13 and 14 are obtained at different strain rate and different rolling directions. The fracture mechanism of the sheet metal are characterised and identified within the figures. The observation indicates that within the lower strain rate, the cracks became a more dominant characteristic meanwhile as the void nucleation and dimples became a more dominant characteristic as the strain rate increased. This mechanism had been notified by Han and Margolin [17] that indicates ferrite -martensite decohesion closer to the fracture strain at lower strain rates. Micrograph indicates voids nucleation being more apparent that the void nucleates within the vicinity of the crack and presumed to be due to the enhanced stress triaxiality near the fracture as had been observed also by N. Pathak [18]. The linking behaviours of the fractures can be observed clearly within Figures 13 and 14 as the fracture begins to coalesce. It indicates that as more number of voids within the vicinity, it allows the cracks to propagate and form and irregular cracking path which is a clear characteristic ductile failure thus that would cause the fracture. As shown in Figure 13(b), the crack propagation could be clearly identified as it occurs along the shear flow lines which evidently causes the specimen to debond and initiate the crack within a zig-zag pattern which indicates a characteristic of ductile failure
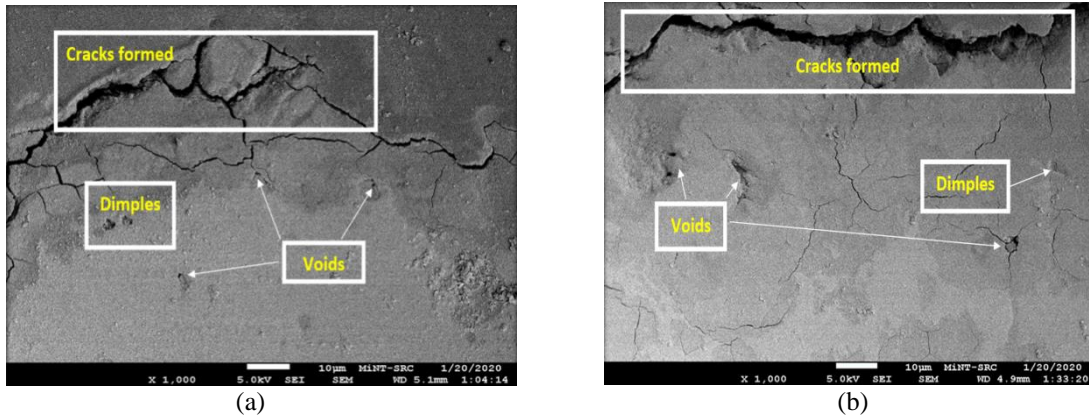
Fig. 13 - SEM micrograph for DP 590 at 1×10^{-3} strain rate at different direction: (a) Longitudinal; (b) Transverse
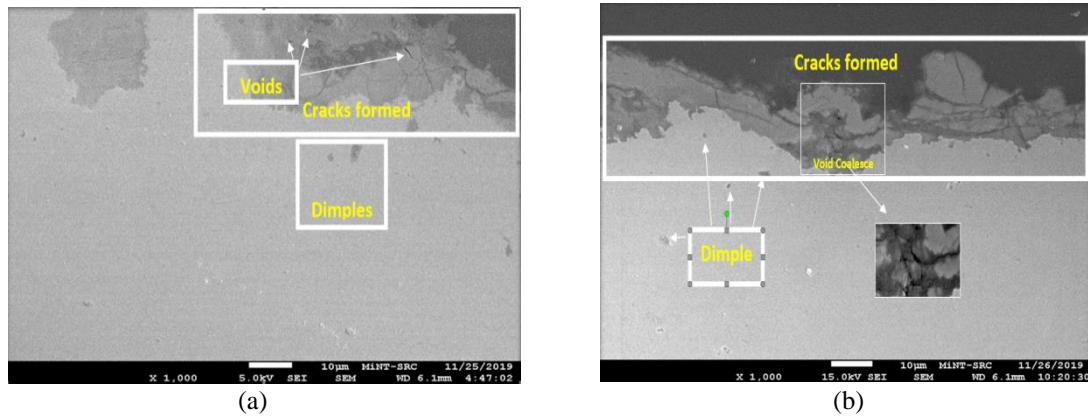

Fig. 14 - SEM micrograph for DP 590 at 1×10^{-1} strain rate at different direction: (a) Longitudinal; (b) Transverse

.

Figure 13 captures clearly the fracture mechanism at lower cross head speed for the material cracks and creeping behaviour of the specimen. Meanwhile in Figure 14, the specimen's microcracks and creep progression are not as pronounced as those specimens at lower strain rate as this suggests that at higher strain, the instantaneous behaviour of the fracture cause the cracks not able to linked with other voids that tends to be more apparent as the number of voids are reduced within the higher cross head speed. In accordance to the data shown in the Figure 13, It suggests that the correlation of the number of voids and the average size of the voids would affect the behaviour of the fracture as larger void size and lower void numbers would behaves with an increment in ductility and strength as suggested in [19] which agrees upon their observations.

4. Conclusion

The paper analyses the effects of different orientations and strain rates to the microstructure and mechanical strength of Advanced High Strength Steel (AHSS) DP590. The data shows that the mechanical properties of such material are sensitive to the changing of strain rate. To be specific, the Elastic Modulus (E), Yield Strength (σ_y) and Ultimate Tensile Strength (UTS) are increased with the increasing strain rate. This is supported by the respective microstructural data obtained from SEM analysis as documented in Figure 6 to 14. In terms of material direction, it can be observed that the longitudinal rolling direction has better mechanical properties compared to the transverse direction.

Acknowledgement

References

[1]   Mohd Nor, M. K., Modeling of Constitutive Model to Predict the Deformation Behaviour of Commercial Aluminum Alloy AA7010 Subjected to High Velocity Impacts, ARPN Journal of Engineering and Applied Sciences, Vol. 11(4), pp. 2349–2353, 2016b

[2]   Mohd Nor, M. K., Ma'at, N., Ho, C. S. (2018), "An Anisotropic Elastoplastic Constitutive Formulation Generalised for Orthotropic Materials", Continuum Mechanics and Thermodynamics, Springer Berlin Heidelberg, 30(4), 825-860 https://doi.org/10.1007/s00161-018-0645-7

[3]   R. Vignjevic, N.K. Bourne, J.C.F. Millett, T. De Vuyst "Effects of orientation on the strength of the aluminum alloy 7010-T6 during shock loading: experiment and simulation" J. Appl. Phys., 92 (8) (2002), pp. 4342-4348

[4]   Sinha, S. and Ghosh, S. (2006), "Modeling cyclic ratcheting based fatigue life of HSLA steels using crystal plasticity FEM simulations and experiments", International Journal of Fatigue, vol. 28, no. 12, pp. 1690-1704

[5]   Mohd Nor M. K., Vignjevic R., Campbell J., Plane-Stress Analysis of the New Stress Tensor Decomposition, Applied Mechanics and Materials, Vol. 315 (2013b), pp 635-639

[6]   Mohd Nor, M. K., Mohamad Suhaimi, I., Effects of Temperature and Strain Rate on Commercial Aluminum Alloy AA5083, Applied Mechanics and Materials, Vol. 660 (2014), pp 332-336

[7]   Ma'at, N., Mohd Nor, M. K., Ho, C. S., Abdul Latif, N., Ismail, A. E., Kamarudin, K. A., Jamian, S., Ibrahim@Tamrin, M. N., Awang, M. K. (2019), "Effects of Temperature and Strain Rates on the Mechanical Behaviour of Commercial Aluminium Alloy AA6061", Journal of Advanced Research in Fluid Mechanics and Thermal Sciences, Vol. 54, no. 1, pp. 21-26

[8]   Smallman, R.E., (1985), "Modern Physical Metallurgy", fourth ed. Butterworths, London.

[9]   Gray, G.T., Bourne, N.K., Millett, J.C.F., (2003), "Shock response of tantalum: lateral stress and shear strength through the front", Journal of Applied Physics 94(10), 6430–6436.

[10]   Mohd Nor M. K., Vignjevic R., Campbell J., Modelling of Shockwave Propagation in Orthotropic Materials, Applied Mechanics and Materials, Vol. 315 (2013a), pp 557-561

[11]   Mohd Nor, M. K. (2015), "The Development of Unique Orthogonal Rotation Tensor Algorithm in the LLNL-DYNA3D for Orthotropic Materials Constitutive Model", Australian Journal of Basic and Applied Sciences, Vol. 9(37), pp 22-27

[12]   Mohd Nor, M. K., Modelling Inelastic Behaviour of Orthotropic Metals in a Unique Alignment of Deviatoric Plane within the Stress Space, International Journal of Non-Linear Mechanics 87, pp. 43–57, 2016a.

[13]   G. B. O. H. D. Espinosa, "Shear and tensile plastic behaviour of austenitic steel TRIP-120 compared with martensitic steel HSLA-100," pp. 187–204, 2010

[14]   Vignjevic, R., Bourne, N. K., Millett, J. C. F. and De Vuyst, T. (2002), "Effects of orientation on the strength of the aluminum alloy 7010-T6 during shock loading: Experiment and simulation", Journal of Applied Physics, vol. 92, no. 8, pp. 4342-4348.

[15]   M. Y. Demeri, Advanced High-Strength Steels: Science, Technology, and Applications. ASM International, 2013

[16]   Ghadbeigi, H., Pinna, C., & Celotto, S,2013. "Materials Science & Engineering A Failure mechanisms in DP600 steel : Initiation , evolution and fracture." ,Materials Science & Engineering A, 588, 420–431.

[17]   Han, S.K.; Margolin, H. Void formation, void growth and tensile fracture of plain carbon steel and a dual-phase steel. Mater. Sci. Eng. A 1989, 112, 133–141

[18]   Pathak, N., Butcher, C., Worswick, M. J., Bellhouse, E., & Gao, J. (2017). Damage Evolution in Complex-Phase and Dual-Phase Steels during Edge Stretching. Materials (Basel, Switzerland), 10(4), 346. https://doi.org/10.3390/ma10040346

[19]   M. F. A. Ibrahim, S. R. S. Bakar, A. Jalar, N. K. Othman, J. Sharif, A. R. Daud, and N. M. Rashdi, "Effect of Porosity on Tensile Behaviour of Welded AA6061-T6 Aluminium Alloy," Appl. Mech. Mater., vol. 66–68, pp. 534–539, 2011

[20]   Kim, Junehyung & Chung, Kyung-Hwan & Lee, Wonoh & Kong, Jinhak & Ryu, Hansun & Kim, Daeyong & Chongmin, Kim & Wenner, Michael & Chung, Kwansoo. (2009). Optimization of Boost Condition and Axial Feeding on Tube Bending and Hydro-Forming Process Considering Formability and Spring-Back. Met. Mater. Int. 15. 863-876. 10.1007/s12540-009-0863-9

[21]   Kim, J. S., Kim, S. I., & Choi, S. H. (2013). Effect of the initial texture components of hot-rolled BH steel on the evolution of deformation texture and stored energy during the cold-rolling process. Metals and Materials International, 19(4), 759–765. doi:10.1007/s12540-013-4015-5

[22]   Baufeld, Bernd. (2009). Mechanical properties of Ti-6Al-4V specimens produced by shaped metal deposition. Science and Technology of Advanced Materials